



Original article

Hydrogel-based matrices for controlled drug delivery of etamsylate: Prediction of *in-vivo* plasma profiles

Soha M. El-Masry^a, Sally A. Helmy^{a,b,*}^a Department of Pharmaceutics, Faculty of Pharmacy, Damanhour University, Damanhour, Egypt^b Department of Clinical and Hospital Pharmacy, Faculty of Pharmacy, Taibah University, AL-Madinah AL-Munawarah, Saudi Arabia

ARTICLE INFO

Article history:

Received 19 September 2020

Accepted 31 October 2020

Available online 6 November 2020

Keywords:

Etamsylate

Controlled release

In-vitro drug release

In-vivo prediction

Convolution

ABSTRACT

Objectives: To design oral controlled release (CR) hydrogel matrix tablets of etamsylate using various hydrophilic polymers. Additionally, to predict plasma concentration-time profiles of etamsylate released from different CR matrices.

Methods: Characterization of the *in-vitro* release rate was performed by various model dependent and model independent approaches. A simple numerical convolution strategy was adopted to predict the *in-vivo* performance of all matrices from their *in-vitro* percent released data. The statistical analysis was conducted utilizing a student *t*-test and ANOVA.

Results: The release of etamsylate from all matrices showed a deviation from Fickian transport mechanism except; F2 followed Case II release whereas, F9 and F11 obeyed Fickian diffusion. CR hydrogel based-matrices (F4 and F11) demonstrated the maximum drug retardation and satisfied the USP release limits. Concentration–time profiles of etamsylate were predicted successfully from the *in-vitro* release data of all prepared matrices. Pharmacokinetic parameters of etamsylate CR hydrogel matrices were significantly changed with comparison to reference product except F1.

Conclusion: The designed (F2–F11) matrices had the capability to extend the plasma level of etamsylate for an adequate time. However, F4 and F11 were considered the most ideal formulations for once daily application of etamsylate. The prediction of *in-vivo* pharmacokinetics of etamsylate was very useful to assess the rationality of the designed matrices for the practical application in humans.

© 2020 The Authors. Published by Elsevier B.V. on behalf of King Saud University. This is an open access article under the CC BY-NC-ND license (<http://creativecommons.org/licenses/by-nc-nd/4.0/>).

1. Introduction

Etamsylate is a hemostatic and non-thrombogenic drug used for treatment and prevention of pre-, per-, or post-surgical capillary hemorrhage (Garay et al., 2006). It acts by inhibition of Prostacyclin I2 synthesis which is responsible for platelet disaggregation (Schulte et al., 2005). Furthermore, it increases the capillary endothelial resistance and promotes the platelet adhesion (Garay

et al., 2006). Etamsylate is completely absorbed from the gastrointestinal tract with oral bioavailability of almost 100% (EMA, 1998). Its peak plasma concentration achieved after three to four hours with a relatively short half-life (EMA, 1998). It is excreted unchanged, largely by the urinary route (Garay et al., 2006). The recommended oral dose of immediate release etamsylate formulation is 500 mg 3–4 times/day during menstruation (Garay et al., 2006). To control hemorrhage before and after surgery, the recommended dose is 250–500 mg 4–6 hourly as needed (Garay et al., 2006). Therefore, a dosage regimen of 3–4 times per day is needed to keep the plasma concentrations of etamsylate above its minimum effective concentration. Accordingly, it is desirable to develop a new formulation of etamsylate in order to extend its clinical effects and decrease the incidence and intensity of adverse events and the dosing frequency for better patient adherence.

In-vitro dissolution is believed to be a fundamental quality assurance test for batch-to-batch uniformity. It suggests that each dosage form unit will has consistent *in-vivo* behavior. Moreover, it can act as a surrogate for *in-vivo* performance (Helmy and ELBedaiwy, 2016). Various studies have been recently published

* Corresponding author at: Department of Pharmaceutics, Faculty of Pharmacy, Damanhour University, Damanhour, Egypt; Department of Clinical and Hospital Pharmacy, Faculty of Pharmacy, Taibah University, AL-Madinah AL-Munawarah, Saudi Arabia.

E-mail addresses: sallyhelmy@pharm.dmu.edu.eg, shelmy@taibahu.edu.sa (S.A. Helmy).

Peer review under responsibility of King Saud University.



Production and hosting by Elsevier

using dissolution testing as a successful measure for mimicking *in-vivo* plasma concentrations (Hidekatsu et al., 2007). Convolution computations are utilized for this purpose (Paroëiæ et al., 2007). Several models have been used ranging from a simple models which suppose that the release or dissolution data of a certain drug exactly mimics its *in-vivo* performance (Hussein and Friedman, 1990; Mojaverian et al., 1992; Hwang et al., 1995; Polli et al., 1996; Bendas, 2009), to more complicated ones that explicit a more complex relationship (Dunne et al., 1997; Ginski and Polli, 1999).

Hydrophilic polymer matrix systems are attractive approaches generally used for designing oral controlled-release (CR) formulations in light of their broad regulatory acceptance, simple manufacturing, cost effectiveness, and flexibility to allow a desirable release pattern (Alderman, 1984; Salsa et al., 1997; Juarez et al., 2001). An extensive research was performed about CR formulations of etamsylate in the world's recognized databases such as; Web of Science, Scopus, Springer, and PubMed. The search was not limited by any period. To the best of our knowledge, no studies have been found about the CR formulations of etamsylate or the formulation of etamsylate in general. Accordingly, the aim of the present research was to design and optimize hydrogel-based matrix CR formulations using various hydrophilic polymers to control etamsylate release. The *in-vitro* release characteristics of etamsylate-containing hydrogel matrices were studied using different model dependent and model independent approaches. Moreover, the research was extended to predict the *in-vivo* performance of etamsylate released from CR matrices utilizing a simple numerical convolution strategy to assess rationality of the designed CR matrices for the practical application in humans.

2. Materials and methods

2.1. Materials

Etamsylate was purchased from Sigma–Aldrich Co., St. Louis, MO, USA. Dicynone[®] tablets (500 mg etamsylate) was purchased from local market (OM Pharma, Geneva, Switzerland). Carbopol was obtained from Lubrizol Advanced Materials, India. Microcrystalline cellulose (MCC) from Hercules Inc., Wilmington, MA, USA. HPMC K4M and HPMC K15M were purchased from Sigma Aldrich, Germany. Sodium alginate and xanthan gum were obtained from Loba Chemicals, Mumbai, India. Magnesium stearate, starch and talc were purchased from Triveni Interchem, India.

2.2. Methods

2.2.1. Formulation of CR hydrogel-based matrix tablets of etamsylate

Etamsylate-containing matrix tablets were designed using various release retarding polymers such as; hydroxypropyl methylcellulose (HPMC) with two viscosity grades (K4M, and K15M),

Carbopol, sodium alginate, xanthan gum, and MCC. The drug and polymers were sieved and mixed thoroughly. After that, magnesium stearate, starch, and talc were finally added to the previous mixture. The ingredients were mixed again for five minutes and compressed using a 12-station single punch tablet machine (Erweka tablet machine, Germany) using round and flat face of 12-mm diameter. All formulations (F1–F11) contain 500 mg etamsylate. The composition of the prepared hydrogel matrices was listed in Table 1.

2.2.2. Evaluation of powder blend

Prior to compression, the powder blend was assessed for angle of repose, bulk density, tapped density, compressibility index (CI) and Hausner ratio (HR) (Carr, 1965; Shah et al., 2008).

Angle of repose (θ) expresses the flowability of powders. It was measured by the fixed funnel and free-standing cone method (Gohel et al., 2007). It was calculated using Equation (1) (Eq. (1)), where h and r were the height and radius of the powder cone, respectively.

$$\tan \theta = h/r \quad (1)$$

Compressibility index (CI) is a measure of strength and stability whereas, Hausner ratio (HR) is a measure of the interparticulate friction (Kumar et al., 2001). Lower CI or lower HR values indicates better flow properties than higher ones. Bulk density (BD) and tapped density (TD) were determined by the graduated cylinder method to calculate CI and HR by Eqs. (2) and (3), respectively.

$$\text{Compressibility index (CI)} = \frac{TD - BD}{TD} \times 100 \quad (2)$$

$$\text{Hausner ratio (HR)} = \frac{BD}{TD} \quad (3)$$

2.2.3. Evaluation of the prepared CR hydrogel-based matrix tablets

After compression, formulated matrix tablets were tested for weight uniformity, drug content, hardness, thickness, friability, and swelling index determination (BP, 2004; USP-NF, 2014). Weight variation was evaluated by weighing of 20 tablets using an electronic balance (Sartorius, Germany). The tablets complies with USP specifications if no more than two tablets are outside the limit and no tablet varies by more than double the limit (USP-NF, 2014). For drug content consistency, 10 tablets were haphazardly selected, weighed and grinded (USP-NF, 2014). A precise amount of this powder was dissolved in 0.1 N HCl and measured utilizing UV-spectroscopy (Agilent Cary 60 UV-Vis Spectrophotometer, Malaysia) at 309 nm. The crushing strength and friability of 10 tablets were assessed by hardness and friability testers (Colpey, Nottingham, NG4 2JY, UK), respectively.

The swelling behavior of the optimized matrices (F4 and F11) was determined in triplicate. It was calculated for both formulations according to method published before (Dorozynski et al.,

Table 1
Compositions of different formulations of etamsylate CR hydrogel matrix tablets.

Ingredients (mg)	F1	F2	F3	F4	F5	F6	F7	F8	F9	F10	F11
Etamsylate	500	500	500	500	500	500	500	500	500	500	500
HPMC K15	–	–	200	300	–	–	100	–	–	–	–
HPMC K4	150	300	–	–	–	–	–	–	–	–	–
Carbopol	–	–	–	–	100	200	100	100	200	–	–
Sodium alginate	–	–	–	–	–	–	–	50	50	–	–
Xanthan gum	–	–	–	–	–	–	–	–	–	100	200
MCC	–	–	–	–	–	–	–	–	–	380	280
Starch	330	180	280	180	380	280	280	330	230	–	–
Magnesium stearate	10	10	10	10	10	10	10	10	10	10	10
Talc	10	10	10	10	10	10	10	10	10	10	10

2004; DiColo et al., 2006; Tadros, 2010). Briefly, the matrix tablet was weighed and placed into 200 mL glass beaker containing 0.1 N HCl, kept up at $37 \pm 0.5^\circ\text{C}$. At predetermined time periods, tablet was taken away and weighted again after the removal of the surplus liquid at the tablet's surface (Venugopalarao et al., 2013). The swollen tablet was then re-weighed. The Swelling index (SI) was calculated using Eq. (4).

The swelling index (SI)

$$= \frac{\text{Weight of swollen tablet} - \text{Initial weight of the tablet}}{\text{Initial weight of the tablet}} \times 100 \quad (4)$$

2.2.4. Differential scanning calorimetry (DSC)

Thermal behavior of etamsylate, polymers and physical mixtures of the optimized matrix tablets (F4 & F11) were monitored using Perkin Elmer Pyris 6 DSC (Shelton, CT, USA). This was to study the compatibility between etamsylate and selected polymers (HPMC K15M, xanthan gum, and MCC). Samples were loaded into an aluminum crimp cell and heated at $10^\circ\text{C}/\text{min}$ ($30\text{--}300^\circ\text{C}$) under nitrogen ($20\text{ mL}/\text{min}$).

2.2.5. Fourier transform infrared (FT-IR) spectroscopy

FT-IR spectra of etamsylate, polymers and physical mixtures of the optimized matrices (F4 & F11) were recorded using FT-IR spectrophotometer of Perkin Elmer version 10.5.3 (Liantrisant, England). The sample was mixed with crystalline potassium bromide and compressed for 5 min to form a disk before scanning from 4000 to 450 cm^{-1} .

2.2.6. Scanning electron microscopy analysis (SEM)

Surface morphologies and porous structures of the optimized hydrogel CR matrices (F4 & F11) were examined after 2 h of dissolution in 0.1 N HCl using SEM (JEOL, JSM- 5200LV, Japan) at 25 kV. Tested samples were coated with gold in a SPI- Module™ Vac/Sputter before SEM analysis.

2.2.7. In-vitro release studies

Etamsylate release from reference tablet (R) and CR hydrogel-based matrix tablets (F1-F11) was conducted utilizing USP Dissolution Testing Apparatus II (paddle method) (Copley Scientific Dis 6000 dissolution system, Nottingham, UK). The release test was carried out using 900 mL of 0.1 N HCl (pH 1.2) for 12 h, at $37^\circ\text{C} \pm 0.5^\circ\text{C}$ and 75 rpm. Samples (5 mL) were taken periodically and filtered immediately ($0.45\ \mu\text{m}$ Millipore filter, Merck KGaA, Darmstadt, Germany). The study was conducted in triplicate. Samples were measured using a UV/Visible spectrophotometer (Agilent Cary 60 UV-Vis Spectrophotometer, USA) set at 309 nm. Release profiles were plotted as the percentage (%) cumulative etamsylate released versus time.

2.2.8. Kinetics of drug release

2.2.8.1. Model dependent in-vitro release characterization. Different kinetic models have been utilized to characterize the in-vitro release data of etamsylate from CR hydrogel-based matrix tablets. Correlation coefficient (r) was calculated. The kinetic model with the highest “ r ” value was considered more appropriate.

Zero-order release model was followed when the release of a drug was independent on its concentration (Costa and Lobo, 2001). % cumulative etamsylate released was plotted against time. This model was represented as in Eq. (5), where C was the % drug released at time t , and k_0 was the zero-order rate constant.

$$C = k_0 t \quad (5)$$

First order release model described the rate of drug release when it was concentration dependent (Costa and Lobo, 2001). Log % of etamsylate remaining was plotted vs. time. It could be represented by Eq. (6), where C was the % drug remaining at time t , C_0 was the initial concentration of the drug and k_1 was the first order rate constant.

$$\text{Log } C = \text{Log } C_0 - k_1 t / 2.303 \quad (6)$$

Higuchi model indicated that the mechanism of drug release from a matrix was diffusion controlled (Higuchi, 1963). % cumulative of etamsylate released from each matrix tablet was plotted vs. square root of time. This model could be described according to Eq. (7), where Q was the % cumulative drug released at time t per unit area, and k_H was the Higuchi release constant.

$$Q = k_H t^{1/2} \quad (7)$$

Korsmeyer-peppas model was utilized to find out the mechanism of drug release (Korsmeyer et al., 1983; Peppas, 1985). It was considered if the drug release mechanism deviated from Fick's law and obeyed an anomalous mechanism. Drug release data were fitted using the following equation (Eq. (8)):

$$M_t/M_\infty = k_{KP} t^n \quad (8)$$

where M_t/M_∞ was a fraction of drug released at time t , k_{KP} was Korsmeyer-peppas release rate constant, and n was the diffusional exponent or drug release exponent which characterized the diffusion release mechanisms from the spherical and cylindrical shaped matrices. For spherical shaped matrices, a value of $n < 0.43$ indicated Fickian diffusion; $0.43 < n < 0.85$ indicated non-Fickian or anomalous diffusion; $0.85 < n < 1$ indicated case II release; and $n > 1$ indicated super case II release (Ritger and Peppas, 1987; Siepmann and Peppas, 2001).

Hixson-Crowell model described the drug release when there was a change in surface area and diameter of particles or tablets (Siepmann and Siepmann, 2013). % drug released was plotted as the cube root of the % of etamsylate remaining in the various CR etamsylate-containing hydrogel-based matrices vs time (Eq. (5)).

$$W_0^{1/3} - W_t^{1/3} = k_{HC} t \quad (9)$$

where W_0 was the initial amount of drug in the CR matrices, W_t was the amount of drug at time t and k_{HC} was Hixson-Crowell constant which described surface volume relation. When “ r ” value of Hixson-Crowell model was higher, a change in the surface area of matrix tablet during the release process had a significant effect on etamsylate release.

2.2.8.2. Model-independent in-vitro release characterization. The release of etamsylate from all the CR hydrogel matrices were compared utilizing the following release parameters: time required for mean dissolution time (MDT), and mean residence time ($\text{MRT}_{\text{in-vitro}}$) of etamsylate in the CR hydrogel matrices, 25%, 50%, and 80% of the drug release ($T_{25\%}$, $T_{50\%}$, and $T_{80\%}$), area under the cumulative release curve (AUCC), and dissolution efficiency (DE) at 6 h and 12 h (Khan, 1975; Podczeczek, 1993; Costa and Lobo, 2001).

The sameness between two release profiles were evaluated by difference factor (f_1) and similarity factor (f_2) (Moore and Flanner, 1996; Costa, 2001). Calculations were performed by Excel add-in DDSolver (Zhang et al., 2010). The differences for $T_{25\%}$, $T_{50\%}$, and $T_{80\%}$, DE, MDT, and MRT were statistically evaluated by a student t -test and one-way analysis of variance (ANOVA).

The DE was calculated to assess the release performance of various etamsylate-containing CR hydrogel matrices. DE values at 6 h and 12 h for all matrices were calculated as in Eq. (10), where y was the % etamsylate released at time t .

$$DE = \frac{\int_{t_1}^{t_2} y \cdot dt}{y_{100} \times (t_2 - t_1)} \quad (10)$$

MDT and $MRT_{in-vitro}$ were used to characterize release rate of etamsylate from the CR hydrogel matrices. MDT indicated the retarding efficiency of polymers on etamsylate release rate whereas, $MRT_{in-vitro}$ was the mean residence time of etamsylate in the CR hydrogel matrices (Podczek, 1993). The MDT and $MRT_{in-vitro}$ values were inversely proportional to the release rate. The MDT and $MRT_{in-vitro}$ were calculated by Eqs. (11) and (12), respectively.

$$MDT = \frac{\sum_{j=1}^n t_{jmid} \times \Delta M_j}{\sum_{j=1}^n \Delta M_j} \quad (11)$$

$$MRT_{in-vitro} = \frac{\int_0^t t(100 - y) \cdot dt}{\int_0^t (100 - y) \cdot dt} \quad (12)$$

where j was the release sample number, n was the number of release sample times, t_{jmid} was the time at the midpoint between t_j and t_{j-1} , and ΔM_j was the additional amount of drug released between t and t_{j-1} .

Fit factors (f_1 and f_2) were adopted to establish the similarity of two release profiles of various CR hydrogel matrices of etamsylate (Khan, 1975; Moore and Flanner, 1996; Costa, 2001). The similarity

Blood conc. ($\mu\text{g/ml}$)

$$= \frac{\text{Total amount of drug present in the blood at different times after absorption}}{\text{Vd} \times \text{Bodyweight}} \times 100 \quad (17)$$

of two release profiles was achieved if f_1 values were < 15 (0–15) and f_2 values were > 50 (50–100) (CDER, 1997). f_1 and f_2 were calculated by equations Eqs. (13) and (14), respectively, where t was the time sample index, n was the number of release times, and R_t and T_t were the % etamsylate released at each time point for the reference and test release profiles, respectively.

$$f_1 = \frac{\sum_{t=1}^n (R_t - T_t)}{\sum_{t=1}^n R_t} \times 100 \quad (13)$$

$$f_2 = 50 \times \log \left\{ \left[1 + \frac{1}{n} \sum_{j=1}^n (R_t - T_t)^2 \right]^{-0.5} \times 100 \right\} \quad (14)$$

2.2.9. Stability of hydrogel matrices

Physical stability studies of most satisfactory CR hydrogel matrices (F4 & F11) were carried out according to the International Conference on Harmonization (ICH) guidelines (ICH, 1996; Mathews, 1999). Matrices were sealed in airtight aluminium package and kept in a humidity chamber maintained at relative humidity of 40 ± 2 °C and $75 \pm 5\%$ 3 months. After the predetermined period, the post-compression parameters and drug release were assessed (Patel et al., 2009).

2.2.10. Prediction of human in-vivo profile of prepared CR hydrogel matrices

The *in-vitro* release profiles of all CR hydrogel matrices (F1-F11) were utilized to derive the *in-vivo* concentration-time profiles of etamsylate. This was achieved by a simple numerical convolution method (Qureshi, 2010). The method used reported pharmacokinetic parameters of etamsylate such bioavailability factor (F), elim-

ination rate constant (k_e), and volume of distribution (V_d) (EMA, 1998; Helmy and El Bedaiwy, 2013). A step-by-step procedure was applied using an accessible spreadsheet program. The *in-vitro* release profiles were changed over into discrete dosage portions where, the amount of drug (mg) released within sampling interval was calculated using Eq. (15).

$$\begin{aligned} &\text{Amount of drug (mg) released within sampling interval} \\ &= (\% \text{ drug release} \times \text{Product strength})/100 \end{aligned} \quad (15)$$

The amount of etamsylate released within sampling interval was corrected for bioavailability (F) therefore, the observed amount of drug appeared in blood was estimated using the following equation (Eq. (16)):

$$\begin{aligned} &\text{Amount of drug (mg) corrected} \\ &= \text{Amount of drug (mg) released within sampling interval} \\ &\quad \times F \end{aligned} \quad (16)$$

The elimination phase starts with a first order elimination rate. After that, the blood concentrations equivalent to the total amount of etamsylate in blood at different times after ingestion of a matrix tablet were calculated using Eq. (17).

Etamsylate concentration-time profiles of R and etamsylate-containing CR hydrogel matrices were predicted using a simple numerical convolution method (Qureshi, 2010). Furthermore, various pharmacokinetic parameters of etamsylate such as area under the curve (AUC), area under the first moment curve (AUMC), peak concentration (C_{max}), time to reach peak concentration (T_{max}), and mean residence time ($MRT_{in-vivo}$) were calculated by non-compartmental method (Hedayat, 2012). AUC and AUMC were calculated by trapezoidal rule. $MRT_{in-vivo}$ was calculated as the ratio (AUMC)/(AUC). The published actual data about the concentration-time profile of Dicynon® tablets (R) (500 mg etamsylate) was used to establish the predictability of the convolution method (Helmy and El Bedaiwy, 2013). The prediction of *in-vivo* concentration-time profiles and pharmacokinetics of etamsylate was conducted in triplicate for all CR hydrogel matrices (F1-F11). The statistical analysis was conducted using one-way ANOVA (Minitab, State College, PA, USA). Average absolute percent prediction error (% PE) (Eq. (18)) of no more than 10% for AUC and C_{max} was used to determine the predictability of the method (CDER, 1997; Bendas, 2009).

$$\%PE = \left(\frac{\text{Observed} - \text{Predicted}}{\text{Observed}} \right) \times 100 \quad (18)$$

3. Results and discussion

The present research was conducted to design and characterize CR hydrogel matrices of etamsylate using different hydrophilic polymers. Hydrogel-based matrices of etamsylate was not previously investigated. The prepared formulations were economic

and reproducible at industry level. The physical and *in-vitro* release characteristics of the designed matrices were evaluated. Prediction of plasma drug-concentration profiles from all CR matrices was also reported for the first time in this article. The *in-vivo* performance was predicted employing a simple numerical convolution method. This was applied to assess the appropriateness of the designed matrices for practical application in humans. Additionally, it might help in the selection of the most optimized formulation(s) for final bioequivalence or bioavailability studies.

3.1. Evaluation of the powder blend and prepared tablets

The powder blend of all formulations (F1-F11) was assessed for angle of repose, bulk density, tapped density, CI and HR as listed in Table 2. The bulk density and tapped density were ranged from 0.449 to 0.567 g/mL and 0.604–0.637 g/mL, respectively. The values of CI (%) and HR ranged from 10.76% to 26.75% and 1.12 to 1.36 which revealed a satisfactory compressibility and good flow properties of all formulations (Chateau et al., 2005). The angle of repose values were in the range between 25.04° and 39.01° which indicated good flow properties of all formulations (Staniforth, 2002).

3.2. Evaluation of prepared matrix tablets

Matrix tablets were evaluated for weight uniformity, drug content, hardness, thickness, and friability as tabulated in Table 2. All matrix tablets were complying the pharmacopeial specifications (BP, 2004; USP-NF, 2014). The weight of all matrix tablets ranged from 0.196 g to 0.218 g whilst, the thickness was in the range between 4.597 mm and 5.88 mm. The hardness and friability of the tablets ranged from 4.59 g/cm³ to 5.88 g/cm³ and 0.234% to 0.665%, respectively. A satisfactory drug content was observed among different formulations where it ranged from 98.11% to 101.7%.

The swelling index (SI) of optimized formulations (F4 and F11) were presented in Fig. 1. The swelling ability reflected the adhesion ability of hydrophilic polymers when it came in contact with the simulated gastric fluid. The rate of SI was fast due to the presence of HPMC K15M, xanthan gum, and MCC. Matrix tablets were intact during the time of experiment (12 h); indicating the capability of the tablets to withstand in the GI tract. The maximum swelling

indices of the selected matrices (F4 and F11) were 3.533 and 3.142, respectively achieved after 8 h. This reflected the ability of HPMC K15M, xanthan gum and MCC to enhance the swelling capability of matrix tablets (F4 and F11) when it came in contact with aqueous fluids.

3.3. Differential scanning calorimetry (DSC)

DSC provided a useful information about the reversibility of phase transitions, thermal history and physical properties of the studied samples as well as a direct determination of whether the transition is endothermic or exothermic. Additionally, it investigated the potential interactions between different ingredients in the physical mixtures. The thermograms of pure etamsylate, HPMC K15M, xanthan gum, MCC, and physical mixtures of the optimized formulations (F4 and F11) were shown in Fig. 2.

The unprocessed etamsylate showed a thermal profile of a crystalline anhydrous drug with a single sharp endothermic peak at 133.5 °C, corresponding to its melting point (Fig. 2a) (BP, 2000). The recorded peak correlated well with that reported by other investigators for the same drug (Desai et al., 2003). The melting transition of HPMC K15M was recorded as a broad peak at 82.11 °C (45.01–110.2 °C), corresponding to the moisture loss (Fig. 2b). Similar phenomena were observed for xanthan gum and MCC. The DSC thermogram of xanthan gum exhibited a melting transition at 84.07 °C (45.4–124.3 °C) (Fig. 2c). The thermal profile of MCC showed a broad endothermic characteristic peak at 83.2 °C (39.5–120.2 °C) (Fig. 2d). A similar DSC thermograms were reported and explained for the same polymers (Ford, 1999; Aigner et al., 2011; Ramasamy et al., 2011).

None of the previous polymers exhibited any thermal signals near the melting peak of etamsylate. Therefore, it was probably possible to assess the potential interactions between etamsylate and polymers in physical mixtures of F4 and F11. The thermal profile of physical mixtures of F4 and F11 displayed the same characteristic peak of etamsylate, indicating that the drug maintained its crystalline nature when mixed with polymers (Fig. 2e & f). However, a slight shift in the melting endotherm of etamsylate was noticed. The endothermic characteristic peak of etamsylate was seen biforked at 127.27 °C and sharp at 128.38 °C in case of the physical mixtures of F4 and F11, respectively with an increase in the enthalpy in comparison to that of the unprocessed drug

Table 2

Pre- and post-compression parameters of the prepared etamsylate CR hydrogel matrix tablets.

Parameters	F1	F2	F3	F4	F5	F6	F7	F8	F9	F10	F11		
Pre-compression	Bulk density (kg/m ³)	0.449 (0.01)	0.543 (0.02)	0.539 (0.02)	0.528 (0.01)	0.537 (0.02)	0.513 (0.03)	0.567 (0.01)	0.548 (0.02)	0.529 (0.01)	0.539 (0.03)	0.552 (0.02)	
	Tapped density (g/m ³)	0.613 (0.01)	0.627 (0.01)	0.604 (0.02)	0.615 (0.01)	0.625 (0.03)	0.613 (0.04)	0.637 (0.02)	0.622 (0.03)	0.604 (0.01)	0.628 (0.02)	0.623 (0.01)	
	Compressibility (%)	26.75 (0.3)	13.40 (0.3)	10.76 (0.4)	14.15 (0.4)	14.08 (0.4)	16.31 (0.3)	10.99 (0.6)	11.90 (0.2)	12.42 (0.3)	14.17 (0.5)	11.40 (0.4)	
	Hausner ratio	1.37 (0.02)	1.15 (0.05)	1.12 (0.04)	1.16 (0.02)	1.16 (0.03)	1.19 (0.02)	1.12 (0.05)	1.14 (0.03)	1.14 (0.06)	1.17 (0.04)	1.13 (0.02)	
	Angle of repose	30.01 (0.6)	28.24 (0.4)	25.04 (0.6)	27.79 (0.5)	28.22 (0.16)	29.12 (0.2)	25.56 (0.7)	26.89 (0.8)	28.34 (0.9)	27.80 (0.6)	25.87 (0.4)	
	Post-compression	Weight (g)	0.198 (0.04)	0.196 (0.01)	0.198 (0.01)	0.218 (0.01)	0.201 (0.02)	0.198 (0.05)	0.197 (0.01)	0.197 (0.02)	0.198 (0.01)	0.198 (0.01)	0.198 (0.02)
		Hardness (g/cm ³)	4.823 (0.02)	4.75 (0.07)	5.18 (0.05)	6.098 (0.09)	4.14 (0.2)	4.82 (0.15)	4.25 (0.2)	6.17 0.1)	4.486 (0.1)	4.173 (0.1)	4.16 (0.08)
Thickness (mm)		5.76 (0.9)	4.597 (0.07)	5.78 (0.05)	5.43 (0.06)	5.04 (0.04)	5.66 (0.07)	5.44 (0.06)	5.65 (0.08)	5.75 (0.07)	5.78 (0.07)	5.88 (0.06)	
Friability (%)		0.234 (0.04)	0.245 (0.05)	0.564 (0.09)	0.642 (0.04)	0.564 (0.08)	0.554 (0.08)	0.453 (0.03)	0.654 (0.07)	0.457 (0.06)	0.334 (0.03)	0.665 (0.1)	
Drug Content (%)		101.5 (0.5)	101.7 (1.3)	100.49 (0.6)	99.85 (0.09)	99.87 (0.6)	98.77 (0.2)	101.1 (0.6)	98.11 (0.7)	99.43 (1.2)	100.7 (0.2)	99.10 (0.04)	

Values are presented as the arithmetic mean (SD).

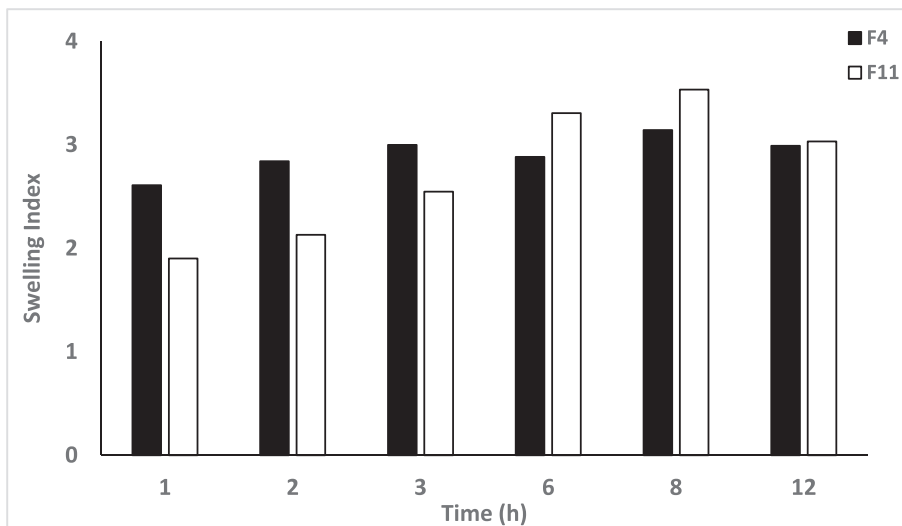


Fig. 1. Swelling index for CR matrix tablets F4 and F10 (n = 3).

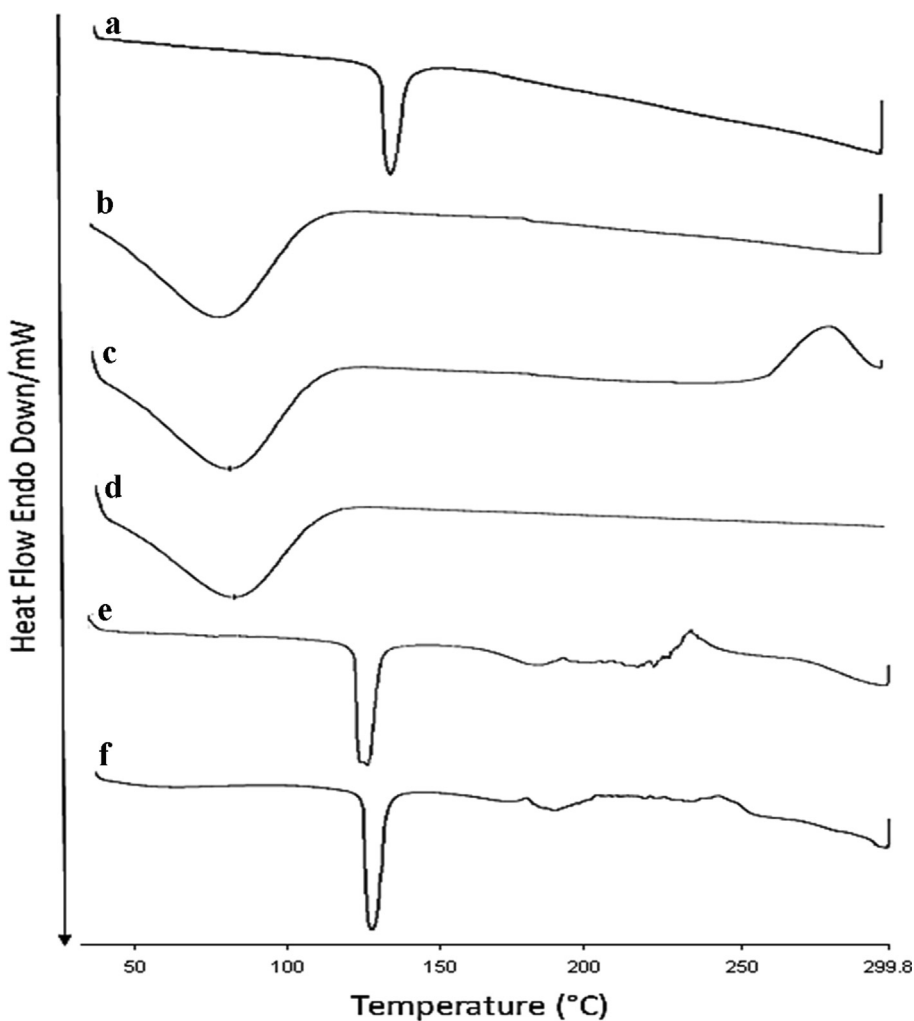


Fig. 2. DSC thermograms of (a) pure etamsylate; (b), HPMC K15, (c) xanthan gum, (d) MCC, (e) physical mixture of F4; and (f) physical mixture of F11.

(Fig. 2e & f). Therefore, the melting signal of etamsylate was preserved, with only minor changes in terms of enthalpy, sharpness or shifting towards lower temperature which cannot be considered

as a sign of an interaction between ingredients. The broad endothermic peak HPMC K15M, xanthan gum, and MCC at ~40–140 °C was nearly disappeared. This might be explained by the

volatilization of the adsorbed water followed by the melting decomposition of polymers. This could indicate the absence of a drug–polymer interaction. FTIR study was performed to confirm the above explanation.

3.4. Fourier transform infrared (FT-IR) spectroscopy

Representative spectra of etamsylate, selected polymers (HPMC K15M, xanthan gum, and MCC) and physical mixtures of optimized matrices F4 and F11 were shown in Fig. 3. The spectrum of unprocessed etamsylate showed an absorption band at 3401 cm^{-1} , 3302 cm^{-1} , 1604 cm^{-1} , and 1447 cm^{-1} for hydroxyl (OH) stretching vibration, amine N–H stretching vibration, C=C stretching frequency, and C–H stretching in the aromatic ring, respectively (Fig. 3a). The biforked peak at 1205 cm^{-1} was related to SO_2 asymmetric stretch with the symmetric stretching being evident at 1082 and 1022 cm^{-1} . The SO_2 bending vibration was clear at 510 cm^{-1} . The peaks corresponding to the N–H wagging were shown as intense peaks at 862 , 824 , 712 and 632 cm^{-1} .

FT-IR spectrum of pure HPMC K15M revealed a peak at 3437 cm^{-1} that was assigned for stretching vibration of OH group whereas, the peak at 2940 cm^{-1} was related to stretching vibration of C–H (Fig. 3b). The peaks corresponding to 1655 and 1060 cm^{-1} was specified to C=C stretching in the aromatic ring and C–O–C

stretching vibration, respectively. The findings concurred with those published earlier (Khanum et al., 2018). FT-IR spectrum of pure xanthan gum recorded a vibration bands for OH group appeared at 3413 cm^{-1} . For the asymmetric- and symmetric-COO- stretching vibrations of pyruvate and glucuronate groups, two peaks at 1621 and 1407 cm^{-1} , respectively were recorded (Fig. 3c). The peak at 1060 cm^{-1} indicated the presence of a C–O–C group. A similar absorption bands were reported previously for the same polymer (Bhat et al., 2014). The pure MCC spectrum revealed several absorption bands which specified for cellulose structure. The peaks corresponding to OH stretching and CH stretching vibrations showed at 3401 cm^{-1} and 2900 cm^{-1} , respectively (Fig. 3d). It showed also absorption bands at 1440 cm^{-1} for CH_2 stretching, and at 1100 – 1400 cm^{-1} for CH, CH_2 , and C–O stretching (Fig. 3d) (Nep and Conway, 2012). The peak at 1691 cm^{-1} might be due to the presence of water (Spoljaric et al., 2009).

Physical mixtures of F4 and F11 showed no evidence of interaction between etamsylate and polymers in F4 and F11 matrices. (Fig. 3e&f). The characteristic absorption bands of etamsylate as well as polymers were present at their usual positions in the FT-IR spectra. The spectrum of each mixture was only a summation of the absorption bands from the individual ingredients. This corroborated the absence of any drug–polymer interaction in F4 and F11 matrices; signifying their mutual compatibility. Thus the FT-IR results were coincided with the DSC results.

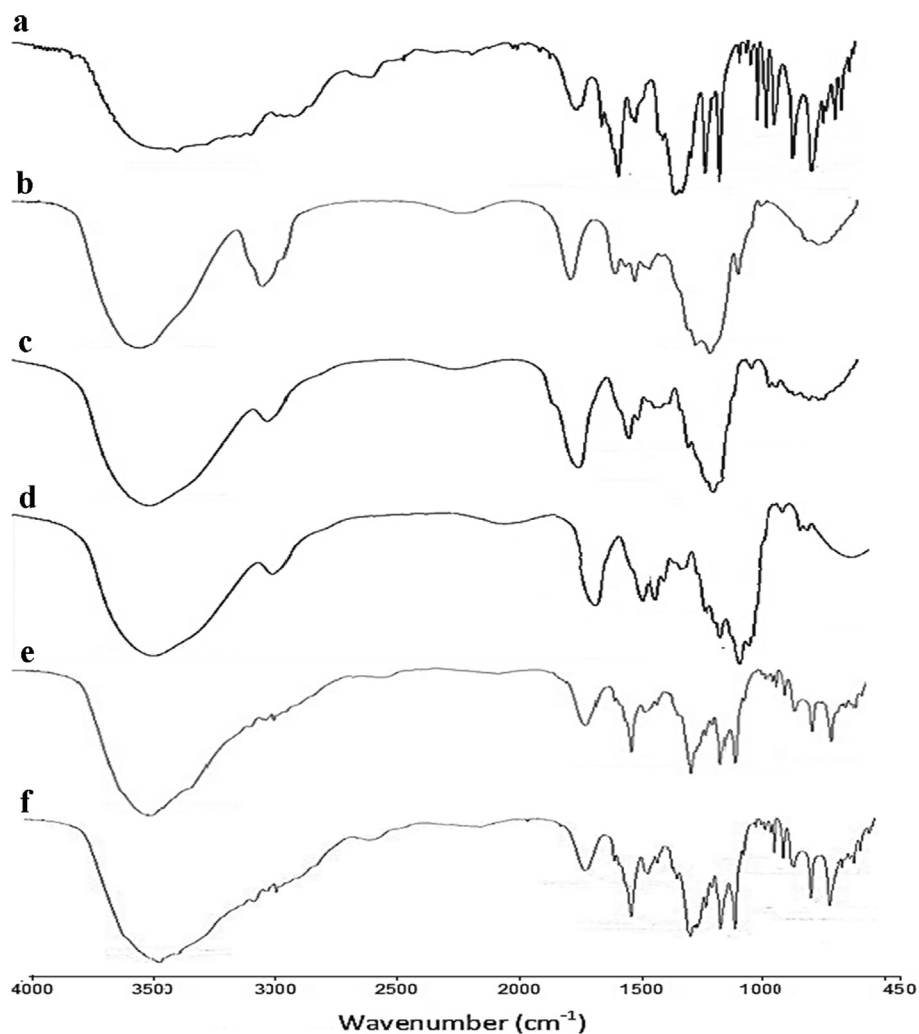


Fig. 3. FT-IR spectra of (a) pure etamsylate; (b), HPMC K15, (c) xanthan gum, (d) MCC, (e) physical mixture of F4; and (f) physical mixture of F11.

3.5. Scanning electron microscopy analysis (SEM)

SEM analysis was performed to determine the surface topography of F4 and F11 hydrogel matrix tablets. Representative SEM photographs F4 and F11 tablets captured after 2 h of dissolution in 0.1 N HCl were represented in Fig. 4. SEM photographs showed many channels and circular pores with different diameters of interconnecting polymeric networks. Soluble drug, such as etamsylate (EP, 2008), could act as a pore former in the matrix tablet in addition to its capacity to form micro-cavities. This could result in the development of a permeable or porous gel layer permitted the release medium to enter the tablet's matrix and move slowly toward tablet's center; hence allowing the diffusion of drug slowly out of the matrix after it came in contact with it (Yang and Fassihi, 1997). Accordingly, the existence of both pores and gelling structure on the tablet surface might indicate the contribution of both diffusion and erosion mechanisms in controlling the release of etamsylate from the optimized CR hydrogel matrix tablets (F4 & F11).

3.6. In vitro release study

The potential mechanisms by which etamsylate was released from hydrophilic matrices could be; (a) diffusion-Fickian release, (b) non-Fickian or anomalous transport (c) zero-order release or

case II mechanism (Ghori et al., 2014). Several release models were used to evaluate the release kinetics of etamsylate release from CR hydrogel matrices as listed in Table 3. The drug release was correlated with numerous mathematical kinetic models. The release pattern of etamsylate from R and different formulated hydrogel matrix tablets was illustrated in Fig. 5. Model independent approaches like MDT, MRT_{in-vitro}, T_{50%}, T_{80%}, DE (6 and 12 h) were assessed for all CR hydrogel matrices (F1-F11) as depicted in Table 4. Furthermore, fit factors (f_1 and f_2) was used to detect the differences between formulations.

All matrix tablets were best fitted to either first order release (Eq. (6)) or Higuchi kinetics (Eq. (7)). The release of R, F1, and F2 was best fitted to first order model whilst, the rest of matrices obeyed Higuchi kinetics (Table 3). To assess the type of release mechanism, release profiles were characterized using Korsmeyer–Peppas model (Eq. (8)) (Korsmeyer et al., 1983). The later was not applicable in case of R and F1 because of fast drug release. The calculated “n” for F2 matrix tablet was 0.865 (0.85 < n < 1); indicating case II (relaxational) release. For hydrogel matrices F3, F4, F5, F6, F7, F8, F10, and F12, the release mechanism obeyed non-Fickian or anomalous release mechanism where, “n” values were 0.838, 0.756, 0.803, 0.678, 0.691, 0.575, and 0.675, respectively (0.43 < n < 0.85) (Table 3). This might indicate the participation of both erosion and diffusion mechanisms in controlling the release of etamsylate from these matrices however, diffusion was

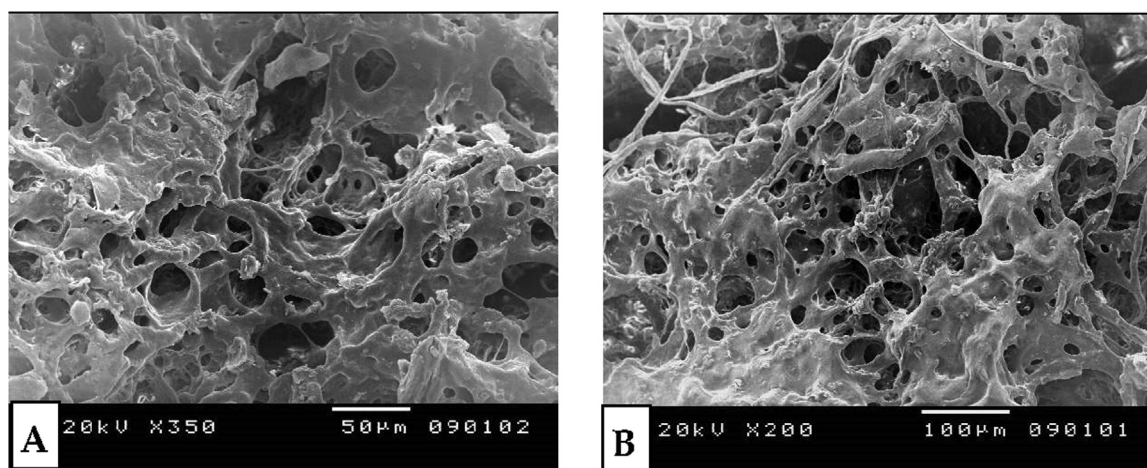


Fig. 4. SEM pictures of (a) F4 and (b) F11.

Table 3 Model dependent in-vitro characterization of etamsylate CR hydrogel matrix tablets.

Formulations	Zero-order (Z-O)		First-order (F-O)		Higuchi matrix (H)		Hixson-Crowell (H-C)		Korsmeyer–Peppas (K-P)			Best Fit	Order of release
	r	k ₀	r	k ₁	r	k _H	r	k _{HC}	r	k _{KP}	n		
R	0.9763	542.05	0.9960	9.79	0.9924	189.02	0.9957	2.768	NA	NA	NA	F-O	NA
F1	0.8246	121.92	0.9997	4.85	0.9590	112.27	0.9569	1.229	NA	NA	NA	F-O	NA
F2	0.9654	93.49	0.9993	1.79	0.9927	82.13	0.9677	0.502	0.9992	109.45	0.865	F-O	Case II
F3	0.9847	17.48	0.9846	0.33	0.9898	35.70	0.9849	0.092	0.9958	23.97	0.838	H, H-C	Non-Fickian
F4	0.9844	9.47	0.8676	0.17	0.9875	26.19	0.9874	0.050	0.9965	14.39	0.756	H, H-C	Non-Fickian
F5	0.9829	35.82	0.9435	0.73	0.9890	52.38	0.9871	0.202	0.9986	48.86	0.803	H	Non-Fickian
F6	0.98791	21.53	0.9886	0.36	0.9903	36.18	0.9810	0.103	0.9988	29.98	0.678	H	Non-Fickian
F7	0.9581	29.73	0.9830	0.53	0.9842	43.69	0.9793	0.150	0.9607	39.71	0.691	H	Non-Fickian
F8	0.9567	25.13	0.9818	0.4	0.9927	43.28	0.9873	0.143	0.9829	41.16	0.575	H	Non-Fickian
F9	0.9586	19.57	0.9863	0.39	0.9968	37.79	0.9818	0.107	0.9936	38.30	0.421	H	Fickian
F10	0.9713	22.61	0.9917	0.51	0.9974	43.07	0.9860	0.138	0.9994	37.55	0.675	H	Non-Fickian
F11	0.9691	18.78	0.9759	0.34	0.9886	35.95	0.9881	0.096	0.9902	32.91	0.424	H, H-C	Fickian

r: correlation coefficient; k₀: zero-order release rate constant (mg%.h⁻¹); k₁: first-order release rate constant (h⁻¹); k_H: Higuchi release rate constant (mg.h^{-1/2}); k_{KP}: Korsmeyer–Peppas release rate constant (h⁻ⁿ); n: Korsmeyer–Peppas release exponent or diffusional exponent; k_{HC}: Hixson–Crowell release rate constant (mg^{1/3}%.h⁻¹).

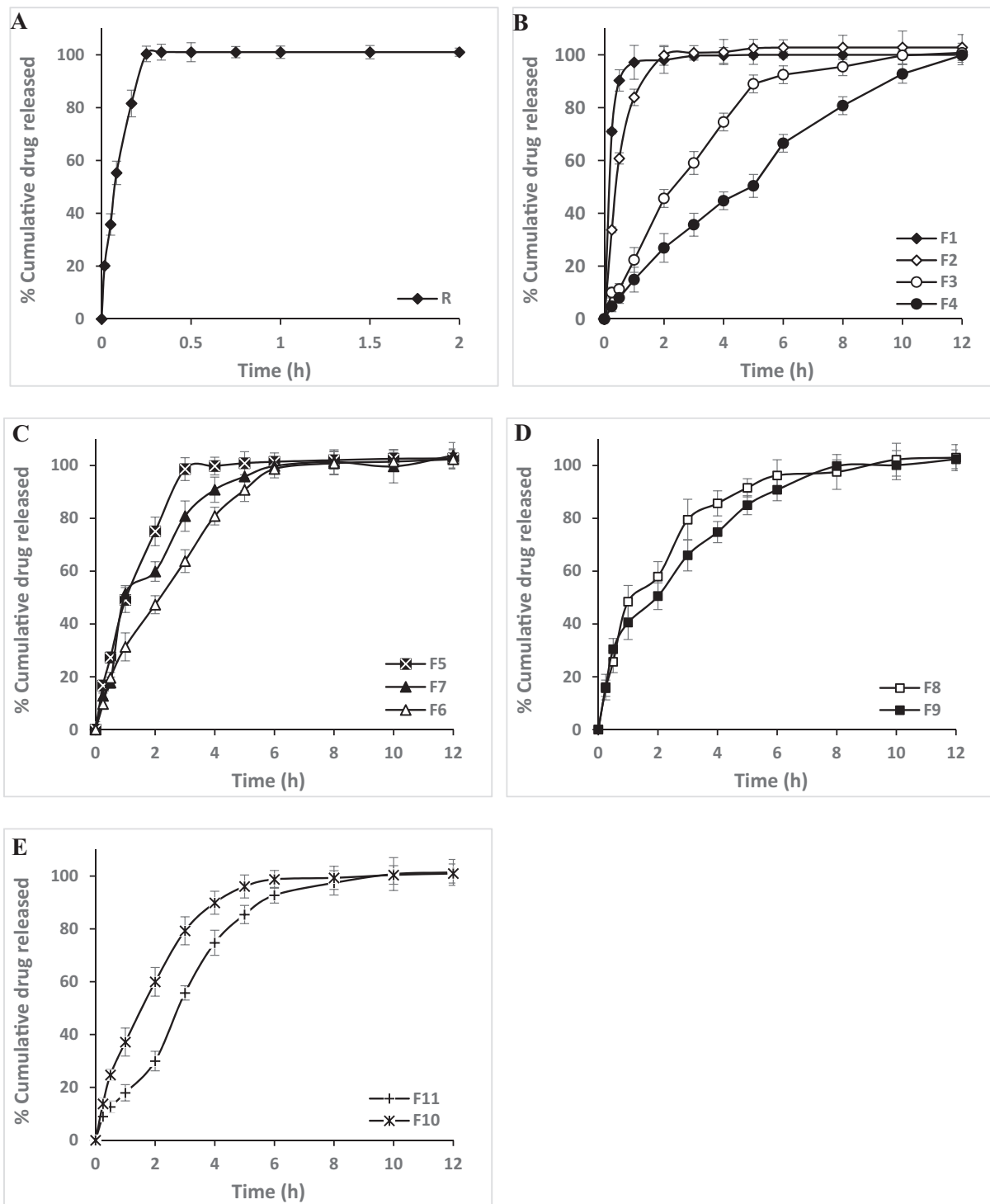


Fig. 5. Release profiles of etamsylate from R and CR matrix tablets (F1-F11) (Mean ± SE, n = 3).

the most dominant mechanism. Whereas, F9 and F11 matrices followed a Fickian diffusion where “n” values were 0.421 and 0.424 ($n < 0.45$); indicating that erosion was the dominated mechanism for F9 and F11 matrices.

HPMC-based matrices have been widely utilized in oral drug delivery systems (Ghori et al., 2014). This could be related to its non-toxic nature, good compression properties, availability in different viscosity grades, as well as good regulatory acceptance (Li et al., 2005). The concentration and viscosity of HPMC played a cru-

cial role in managing the release behavior of etamsylate from hydrophilic matrices. Therefore, their effect on the release of etamsylate from matrix tablets was studied. HPMC K4M (4000 cps) and HPMC K15M (15000 cps) were used in the formulation of (F1 & F2) and (F3 & F4) matrices, respectively (Table 1). The *in-vitro* release profiles of etamsylate from HPMC-based matrices (F1-F4) were illustrated in Fig. 5b.

During release testing, HPMC initially hydrated to form an external gel layer covering the tablet. Subsequently, persistent

Table 4
Model independent in-vitro characterization of etamsylate CR hydrogel matrix tablets.

Formulations	AUC	MRT _{in-vitro}	MDT	T25%	T50%	T80%	DE 6	DE 12
R	190.9 (7.5)	0.07 (0.003)	0.09 (0.005)	0.029 (0.001)	0.071 (0.004)	0.164 (0.008)	–	–
F1	1171.8 (67.3)	0.368 (0.02)	0.281 (0.02)	0.059 (0.004)	0.143 (0.01)	0.332 (0.03)	0.953 (0.008)	0.976 (0.056)
F2	1143.9 (83.7)	0.428 (0.04)	0.560 (0.05)	0.160 (0.008)	0.332 (0.01)	0.896 (0.06)	0.915 (0.02)	0.953 (0.055)
F3	921.7 (38.0)	2.169 (0.1)	2.853 (0.12)	0.490 (0.02)	2.261 (0.07)	5.019 (0.19)	0.563 (0.02)	0.768 (0.025)
F4	719.6 (35.1)	3.437 (0.14)	4.793 (0.1)	0.911 (0.02)	3.644 (0.1)	9.329 (0.28)	0.343 (0.02)	0.599 (0.034)
F5	1081.0 (53.1)	0.497 (0.04)	1.390 (0.06)	0.228 (0.01)	0.911 (0.05)	2.332 (0.19)	0.793 (0.03)	0.900 (0.052)
F6	970.8 (11.6)	1.530 (0.06)	2.512 (0.09)	0.477 (0.02)	1.750 (0.07)	4.480 (0.22)	0.612 (0.03)	0.800 (0.046)
F7	1031.0 (100.0)	1.156 (0.04)	2.065 (0.07)	0.327 (0.01)	1.309 (0.09)	3.352 (0.17)	0.709 (0.02)	0.859 (0.034)
F8	1011.2 (54.7)	1.573 (0.05)	2.179 (0.06)	0.334 (0.030)	1.335 (0.07)	3.417 (0.14)	0.687 (0.03)	0.842 (0.049)
F9	960.3 (26.4)	2.070 (0.1)	2.615 (0.1)	0.437 (0.02)	1.909 (0.04)	4.887 (0.18)	0.608 (0.03)	0.809 (0.019)
F10	1014.5 (53.4)	1.454 (0.1)	1.953 (0.09)	0.337 (0.03)	1.348 (0.07)	3.450 (0.27)	0.692 (0.02)	0.845 (0.048)
F11	940.5 (30.3)	2.141 (0.08)	2.724 (0.17)	0.483 (0.03)	1.934 (0.19)	4.951 (0.22)	0.583 (0.02)	0.783 (0.02)

Values are presented as the arithmetic mean (SD) (n = 3).

AUC: area under the cumulative release curve; MRT_{in-vitro}: mean residence time of the drug substance molecules in the dosage form; MDT: mean dissolution time; T25%: time required for 25% of the drug release; T50%: time required for 50% of the drug release; T80%: time required for 80% of the drug release; DE 6: dissolution efficiency at 6 h; and DE 12: dissolution efficiency at 12 h.

contact with the release medium led to a bulk hydration of the matrix; leading to gel layer formation across the matrix tablet where, HPMC transformed from an amorphous into a rubbery state that eventually, led to HPMC swelling (relaxation), followed by matrix erosion (Ghori et al., 2014). The matrix swelling, diffusion of drug through the gel layer and/or matrix erosion were dependent on the concentration and viscosity of HPMC (Wan et al., 1991; Mitchell et al., 1993; Li et al., 2005). Moreover, drug release rate and mechanism of release were also affected by the concentration and viscosity of HPMC. Furthermore, the tortuosity and porosity of matrices could be considered a definitive features hindering the drug diffusion from the matrix gel layer during dissolution. At more elevated levels of HPMC, the tortuosity of matrices increased whereas, the porosity decreased. The increase in tortuosity might be due to polymer chain entanglement at the outermost layer of matrix tablets which hindered the dissolution of the polymer (Mitchell et al., 1993; Li et al., 2005, Chaibva et al., 2010; Maderuelo et al., 2011). Whilst, the decrease in matrix porosity might be attributable to the low liquid movement across the matrix surface which led to slower drug release rates (Reza et al., 2003).

Referring to the results of HPMC-based matrices (F1 & F2), the increase in the concentration of HPMC in the matrix led to a slower drug release. Matrices with 15% (F1) and 30% (F2) HPMC K4M showed a relatively high release rate where almost a complete etamsylate release were observed after 1 and 2 h, respectively (Fig. 5b). However, a noticeable delayed drug release was observed in case of F2 matrix tablet due to higher HPMC K4M concentration than F1 matrix tablet. The “n” value of F2 (0.865) indicated a case II release where, the release of etamsylate was dependent on purely matrix relaxation or erosion-mediated release mechanism (Table 3). Additionally, the erosion mechanism was visually confirmed by the observed disintegrated particles of HPMC-based matrices (F1 & F2) distributed in the release vessels. Where, HPMC K4M at the surface of the matrix was diluted continuously by the release medium; leading to disentanglement of polymeric chains until the matrix tablet disappeared (Ghori et al., 2014). A statistically significant differences were shown in all the model independent parameters when F1 was compared with F2 as displayed in Table 4. The values of MDT, MRT_{in-vitro}, T_{50%}, and T_{80%} were significantly increased with an excess in the polymer concentration (Table 4). However, the values of DE-6h and DE-12h decreased as the concentration of HPMC K4M increased (Table 4). This was supported by the values of f_1 and f_2 which were 15.25 and 42.08; confirming the difference between F1 and F2 matrix tablets.

The effect of viscosity of HPMC (K4M vs. K15M) on etamsylate release from matrices (F1 & F2 vs. F3 & F4) was also shown in

Fig. 5b. Matrix tablets that contained different concentrations of HPMC K15M (F3 & F4) released etamsylate in significantly longer time periods (Fig. 5b) compared to matrices formulated with HPMC K4M (F1 & F2). The release rate was extended from 2 hrs (30% HPMC K4M; F2) to 12 hrs (30% HPMC K15M; F4) when the viscosity of HPMC was increased from 4000 cps to 15,000 cps, respectively with the same amounts of polymers (Table 1). The model independent approaches showed a statistically significant difference when HPMC K4M (F1 & F2) was compared with HPMC K15M (F3 & F4) as shown in Table 4.

F3 and F4 showed initial burst release of 22.35% and 14.89% during the first hour of the release test, respectively. This might be related to the erosion of the matrix surface of F3 and F4 prior to the formation of gel layer around the core of the matrix tablet (Bendas; 2009). The release of etamsylate from F3 and F4 matrices after 2 hrs were 45.62% and 28.89%, respectively. A complete drug release was achieved after 10 and 12 h in case of F3 and F4, respectively. Increasing the concentration of HPMC K15M from 15% (F3) to 30% (F4) might lead to an increase in the gel viscosity hence, a decrease in etamsylate diffusion from F4 matrix tablet was achieved. In case of F4 (30% HPMC K15M), the drug release extended and the release rate decreased due to an increase in the concentration and viscosity of HPMC. This might be related to the difference in the speed of the gel barrier that was generated after the matrix tablet came in contact with the release medium (Singhvi et al., 2014). Furthermore, the slow-release was probably due to high polymer entanglement, high gel strength, and also to the lower effective molecular diffusional area at high viscosity grade (15000 cps) compared with low viscosity grade (4000 cps) (Table 4 and Fig. 5) (Ford et al., 1985; Shah et al., 1993).

The CR matrix tablets F3 and F4 obeyed both Higuchi and Hixson-Crowell kinetics (Table 3). According to Korsmeyer-Peppas model, it was apparent that as the HPMC concentration in a matrix tablet varied, “n” values changed. Both diffusion and erosion mechanisms were involved in controlling etamsylate release from F3 and F4 matrices (Table 3). The “n” values for F3 and F4 matrices were 0.838 and 0.756 (0.43 < n < 0.85), respectively; indicating a non-Fickian or anomalous diffusion and polymer matrix relaxation or erosion. This could be due to the higher amount of HPMC K15M which formed a strong gel layer quickly which was more resistant to diffusion and/or erosion especially for water soluble drug such as etamsylate (EP, 2008; Mitchell et al., 1993). This phenomenon usually occurs in the oral CR matrix formulations where more than one release mechanism is contributed, such as erosion and swelling (Singhvi et al., 2014). However, the diffusion mechanism was more dominated in F4 than F3 as indicated from the lower “n” value of F4; depending on the

HPMC level and viscosity (Sinha Roy and Rohera, 2002). This was corroborated with that reported previously where, water soluble drugs were released mainly by diffusion through a gel layer before the matrix erodes (Yang and Fassihi, 1997; Bettini et al., 2001; Ghori et al., 2014). Accordingly, the solubility of entrapped drugs was another key factor in evaluating the release behavior from hydrophilic matrices. Hixon-Crowell model was appropriate to reflect the release of etamsylate from CR matrices F3 and F4. This indicated that the change in the diameter and surface area of matrix tablets affected the drug release during the release process.

The above explanation was supported by the values of MDT, $MRT_{in-vitro}$, $T_{50\%}$, and $T_{80\%}$ (Table 4). The values of MDT and $MRT_{in-vitro}$ were significantly increased with an increase in the polymer concentration from 2.853 h to 4.793 h and 2.169 h to 3.437 h in case of F3 and F4, respectively (Table 4). Furthermore, $T_{50\%}$ and $T_{80\%}$ values were also enhanced by an increase of HPMC K15M from 15% to 30% where, they reached 2.261 h to 3.644 h, and 5.019 h to 9.329 h, respectively (Table 4). This indicated the excellent drug retarding capability of HPMC K15M (30%) (Prajapati et al., 2011). The values of DE-6h and DE-12h decreased from 0.563 to 0.343 and 0.768 to 0.599, respectively as HPMC K15M amount increased from 15% to 30% in the formulations F3 and F4, respectively as depicted in Table 4. The values of f_1 and f_2 were 16.01 and 36.08; confirming the difference between F3 and F4. From the previous results, a negligible burst release was noticed (<20% drug release in the first hour) with F4. Furthermore, the release pattern of F4 complied with the USP dissolution limits which were 15–30% at the 2 h, 40–55% after 4 h, 55–70% after 6 h and >95% after 12 h (Sankalia et al., 2008). Thus, 30% HPMC K15M was succeeded to slow the release of etamsylate from the CR matrix tablet F4 which was considered ideal for once daily application of etamsylate.

Another pattern was observed with F5 and F6 when Carbopol was used as the retarding polymer (Fig. 5c). Carbopol is a lightly crosslinked polymer that enables the entrapment of drug in its hydrogel matrix; resulting in a slow drug release profile. The rate and degree of Carbopol swelling were elevated due to the ionization of the carboxylic acid groups (Khan and Jiabi, 1998). The increase in the Carbopol concentrations from 10% to 20% resulted in a slow and extended drug release. F5 and F6 showed an initial burst release of 49.06% and 31.32% during the first hour of the release test, respectively. This might be attributed to incomplete gel barriers of Carbopol matrices; resulting in high initial release of etamsylate. Neither F5 nor F6 followed the USP limits for the percentage release of etamsylate from CR matrices (Sankalia et al., 2008) where the %release after 2hrs was 75.03% and 40.29%, for F5 and F6 matrices, respectively. The release of etamsylate extended from 4 h in the case of F5 to 8 h in case of F6 (Fig. 5c). The CR matrix tablets F5 and F6 followed Higuchi model (Table 3). The “ n ” values for formulation F5 and F6 were 0.803 and 0.678 ($0.43 < n < 0.85$), respectively; indicating a non-Fickian transport. However, the diffusion mechanism was more prevailed in F6 than F5 as indicated from the lower “ n ” value of F6. This could be due to the higher concentration of Carbopol (20%) in F6 which allowed a formation of a more stronger gel layer with a less region of micro-viscosity; as well as closing the micropores in the swollen tablet (Seng et al., 1985).

A significant changes in all the model independent parameters (MDT, $MRT_{in-vitro}$, $T_{50\%}$, $T_{80\%}$, DE-6h, and DE-12h) were observed when polymer concentration changed from 10% to 20% as listed in Table 4. The values of f_1 and f_2 were 15.77 and 40.45; supporting the difference between F5 and F6. The values of MDT, $MRT_{in-vitro}$, $T_{50\%}$, and $T_{80\%}$ were significantly increased with an increase in the Carbopol concentration (Table 4). Conversely, the values of DE-6h and DE-12h decreased as the amount of polymer increased (Table 4). This could be explained by the direct relationship

between Carbopol concentration and the increase in the amount of water uptake which allowed the swelling of tablet matrix and the formation of a thick gel layer controlling the drug release. This could lead to a reduction in the diffusion coefficient of the drug and eventually, a slower release rate (Velasco et al., 1999; Rao et al., 2008).

In an attempt to decrease the initial burst release at the first hour and slow the release of etamsylate from F5, 10% HPMC K15M was added to 10% Carbopol to prepare F7. This was possibly related to the stronger hydrogen bonding between the carboxyl group of Carbopol and the hydroxyl group of HPMC; resulting in a stronger crosslinking between the two polymers and a synergistic increase in viscosity (Samani et al., 2003). Accordingly, a synergistic effect of HPMC-Carbopol combination on the release rate of etamsylate was expected. The CR matrix tablet F7 followed Higuchi model (Table 4). The “ n ” value was 0.691 ($0.43 < n < 0.85$), respectively; indicating a non-Fickian transport. The initial burst release at the first hour decreased from 49.06% to 41.43% in case of F5 and F7, respectively (Fig. 5c) which might be attributed to the addition of HPMC K15M to Carbopol. This addition might overcome the non-fully swollen behavior of Carbopol and its large region of micro-viscosity. However, the release profiles of (F7 vs. F5) and (F7 vs. F6) were relatively the same where f_1 and f_2 values were 9.25 & 53.83 and 8.01 & 55.76, respectively. A significant changes were observed in all the model independent parameters (MDT, $MRT_{in-vitro}$, $T_{50\%}$, $T_{80\%}$, DE-6h, and DE-12h) after the addition of HPMC K15M compared to F5 and F6 (Table 4). The values of MDT, $MRT_{in-vitro}$, $T_{50\%}$, and $T_{80\%}$ were significantly increased after the addition of HPMC K15M compared with F5 whereas, DE-6h and DE-12h decreased (Table 4). The opposite had happened in case of F7, the values of MDT, $MRT_{in-vitro}$, $T_{50\%}$, and $T_{80\%}$ were significantly decreased compared with F6 whereas, DE-6h and DE-12h increased (Table 4). This indicated that HPMC K15M enhanced the release parameters of F5 when added to 10% Carbopol however, F6 with 20% Carbopol alone was the better in controlling etamsylate release than F7.

Sodium alginate is widely used in the formulation of CR hydrophilic matrices due to its hydration and swelling capacities. For controlling the release of etamsylate, 5% of sodium alginate was added to the formula F5 and F6 to form F8 and F9 matrices, respectively (Table 1). This led to slowing the release of etamsylate however, no significant differences observed compared to F5 and F6. The release behavior of etamsylate from F8 and F9 were illustrated in Fig. 5d. Similar release profiles of (F5 vs. F8) and (F6 vs. F9) were obtained where f_1 and f_2 values were 8.36 & 51.88 and 7.24 & 61.74, respectively. The release of etamsylate from F8 matrix tablet showed a deviation from the Fickian transport mechanism ($n = 0.575$) whereas, etamsylate release from F9 tablet matrix followed Fickian transport mechanism ($n = 0.421$). Both formulations showed also burst effect during the first hour of the release. For F8, the values of MDT, $MRT_{in-vitro}$, $T_{50\%}$, and $T_{80\%}$ were increased significantly than F5 where, they reached 2.179 h, 1.573 h, 1.335 h, and 3.417 h, respectively (Table 4). Conversely, for F9, similar values were obtained for the same parameters which were 2.615 h, 2.070 h, 1.909 h, and 4.887 h, respectively (Table 4). Moreover, the release pattern of F7 and F8 did not comply with the USP requirements (Sankalia et al., 2008).

Several trials were done by incorporating xanthan gum with MCC at two concentration levels (10 and 20%) to prepare F10 and F11 matrices, respectively as shown in Table 1. MCC was used in the formulation of etamsylate matrices due to its versatility as a direct compression excipient (Thoorens et al., 2014). Incorporating xanthan gum and MCC in the prepared matrix tablets might led to improve the swelling capability of matrix tablets when it came in contact with aqueous fluids due to increase the water uptake capacity and porosity of matrix (Garg and Gupta, 2009). The %

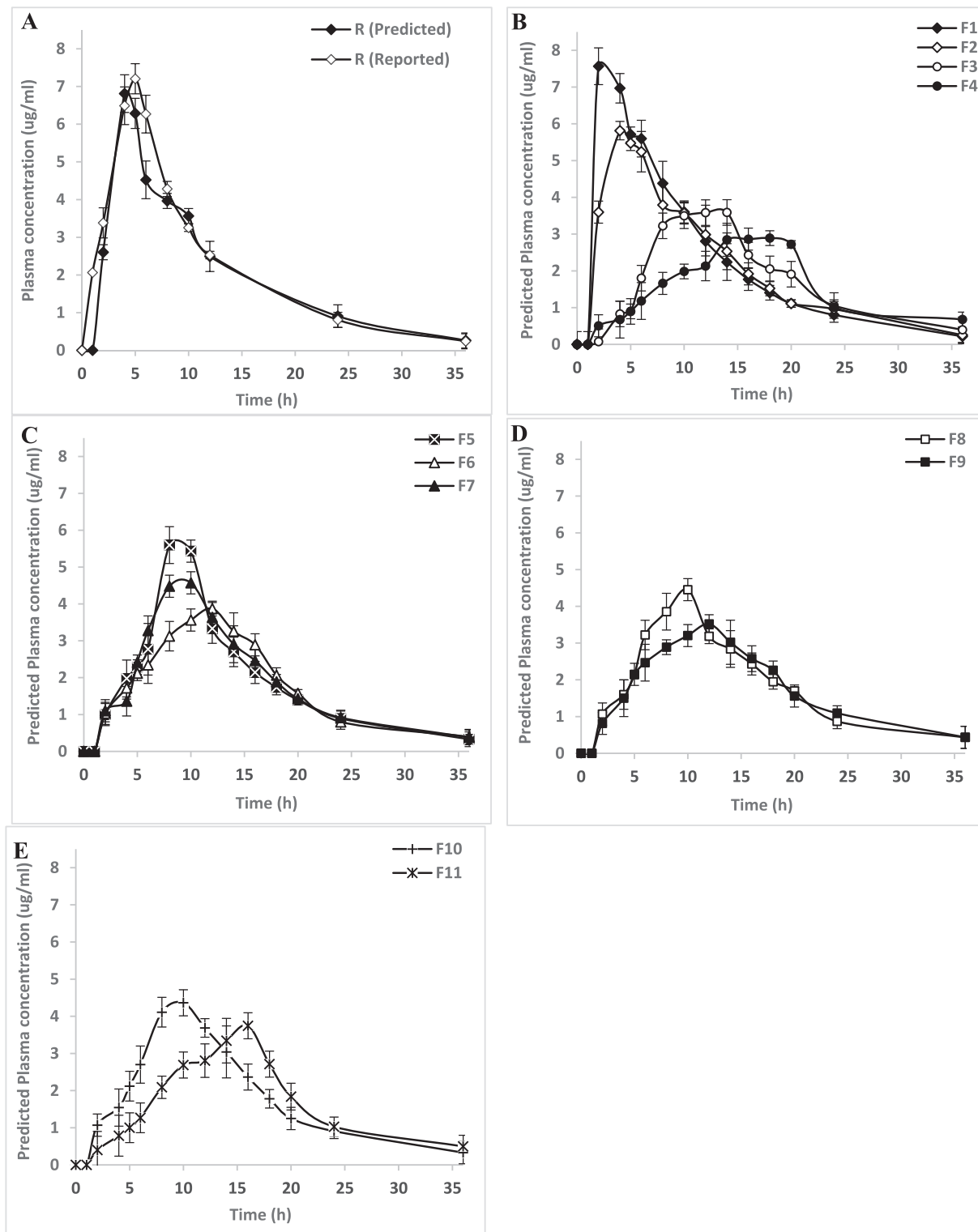


Fig. 6. Predicted plasma drug concentration–time profiles of etamsylate (Mean ± SE, n = 3).

etamsylate released at the first hour was 37.16 and 17.96 from F10 and F11 respectively and 59.97 and 29.98 after 2 hrs from the same matrices respectively as presented in Fig. 5e. The release of CR matrix tablets F10 and F11 obeyed both Higuchi kinetics (Table 3). The calculated “n” value of F10 was 0.675 which indicated non-Fickian (anomalous) release, coupled diffusion-erosion mechanism. However, the “n” value of F11 was 0.424 that reflected Fick-

ian release (Table 3). Matrix tablets prepared with 20% xanthan gum (F11) showed a faster rate of swelling and a lower rate of erosion than those prepared with 10% xanthan gum (F10). This behavior might be related to an increase of water uptake and viscoelastic mass formation (Talukdar and Kinge, 1995). Additionally, F11 followed Hixson-Crowell kinetics (Table 3). This could explain the decrease in the % etamsylate released from F11 compared to F10

Table 5
Predicted pharmacokinetic parameters of etamsylate CR hydrogel matrix tablets.

Formulations	C_{max} ($\mu\text{g/ml}$)	T_{max}^* (h)	AUC ($\mu\text{g/ml}\cdot\text{h}$)	MRT (h)	k_e (h^{-1})	$T_{1/2}$ (h)	
R	Predicted	6.81 (0.538)	4	72.15 (5.18)	9.25 (0.660)	0.097 (0.007)	7.13 (0.639)
	Actual	7.20 (0.684)	5	77.38 (5.557)	8.69 (0.620)	0.098 (0.004)	7.06 (0.633)
F1		7.56 (0.539)	2	79.38 (4.016)	8.63 (0.616)	0.103 (0.007)	6.68 (0.59)
F2		5.81 (0.415)	4	72.64 (5.218)	9.54 (0.681)	0.096 (0.003)	7.16 (0.64)
F3		3.58 (0.256)	14	58.27 (4.183)	12.87 (0.919)	0.092 (0.005)	8.46 (0.759)
F4		2.89 (0.206)	18	53.50 (3.84)	15.22 (1.087)	0.074 (0.006)	9.29 (0.833)
F5		5.59 (0.399)	8	66.09 (4.748)	11.41 (0.815)	0.088 (0.006)	7.81 (0.702)
F6		3.87 (0.276)	12	60.84 (4.37)	12.61 (0.900)	0.079 (0.005)	8.69 (0.86)
F7		4.57 (0.326)	10	64.80 (4.655)	11.84 (0.84)	0.086 (0.006)	8.02 (0.719)
F8		4.45 (0.31)	10	63.05 (4.529)	12.37 (0.883)	0.079 (0.002)	8.75 (0.386)
F9		3.52 (0.25)	12	60.31 (4.33)	12.66 (0.904)	0.078 (0.004)	8.79 (0.788)
F10		4.36 (0.311)	10	61.77 (1.74)	11.78 (0.841)	0.083 (0.006)	8.29 (0.530)
F11		3.74 (0.26)	16	56.17 (1.809)	14.06 (1.004)	0.076 (0.004)	9.02 (0.809)

Values are presented as the arithmetic mean (SD) of the pharmacokinetic parameters (n = 3).

* T_{max} values are presented as median.

during the first hour which might be due to the available surface area that affect the initial amount dissolved from the surface of the prepared formulation.

The MDT, $MRT_{in-vitro}$, $T_{50\%}$, $T_{80\%}$, DE-6h, and DE-12h values were 1.953 h, 1.454 h, 1.348 h, 3.450 h for F10 and 2.724 h, 2.141 h, 1.934 h, and 4.951 h for F11 matrix tablet. Comparing etamsylate release profiles of F10 and F11, the f_1 and f_2 values obtained were 18.29 and 42.54; confirming the difference between F10 and F11. This signified the aptitude of F11 to extend the release of etamsylate furthermore, it satisfied the USP limits for once daily formulation of etamsylate (Sankalia et al., 2008).

Accordingly, the most satisfied and optimized CR hydrogel matrices were F4 and F11. However, the *in-vitro* release data of all etamsylate-containing matrices (F1-F11) were used in the prediction of *in-vivo* performance of etamsylate.

3.7. Stability

No significant differences ($p \geq 0.05$) were observed concerning drug content, drug release profile, and release kinetic of most satisfactory CR hydrogel matrices (F4 & F11); suggesting the reproducibility and stability of etamsylate-containing CR matrices.

3.8. Prediction of human *in-vivo* plasma concentration-time profile of prepared formulations

Prediction of *in-vivo* performance of etamsylate in humans was one of the most important objectives of the *in-vitro* release testing. Moreover, the prediction of *in-vivo* human pharmacokinetics is essential during the drug development. In this study, a simple convolution method was utilized the *in-vitro* release data of R and various CR matrix tablets (F1-F11) to derive the expected *in-vivo* performance of etamsylate (Qureshi, 2010). The method used the reported pharmacokinetic parameters of etamsylate which were V_d (50.8 L), F (1.0) and k_e (0.098 h^{-1}) (Helmy and El Bedaiwy, 2013). Predicted plasma profiles of CR hydrogel matrices of etamsylate were presented in Fig. 6. Various PK parameters such as; C_{max} , AUC, T_{max} , and MRT were calculated by non-compartment modeling as listed in Table 5.

The predicted *in-vivo* profile of R tablet was compared with previously published *in-vivo* profile of etamsylate (Helmy and El Bedaiwy, 2013) as plotted in Fig. 6a. The predicted *in-vivo* curve was similar ($p \geq 0.5$) to the actual *in-vivo* profile. Furthermore, the predicted pharmacokinetic parameters were similar ($p \geq 0.5$) to that of the actual reported data as depicted in Table 5 (Helmy and El Bedaiwy, 2013). The %PE values between actual published data and the predicted value were 5.477% and 6.758% (<15%) for

C_{max} and AUC, respectively; demonstrating the predictability and validity of the method (CDER, 1997). Accordingly, these results showed the ability of the mathematical convolution technique (Qureshi, 2010) to predict the concentration–time profiles of etamsylate from *in vitro* release data of the prepared CR hydrogel matrix tablets.

The C_{max} , T_{max} , k , $t_{1/2}$ of CR hydrogel matrices (Table 5) were found to be significantly changed with comparison to R product except F1. This indicated that the designed (F2-F11) formulation has the capability to extend the plasma level of etamsylate for an adequate time. However, F4 and F11 were considered the most ideal formulations for once daily application of etamsylate.

4. Conclusion

There are as yet no studies that has been published about the CR formulations of etamsylate One of the objectives of this work was to design and characterize a CR hydrogel based-matrices of etamsylate using various hydrophilic polymers. The proposed method of preparation was simple, economic and reproducible. Various model dependent and model independent approaches were utilized for the *in-vitro* characterization of the prepared matrices. The release of etamsylate from all matrices was through a non-Fickian or anomalous transport mechanism, however, Case II release and Fickian diffusion mechanisms were dominated in F2 and F9 & F11 matrices, respectively. CR hydrogel based-matrices (F4 and F11) demonstrated the maximum drug retardation therefore, considered ideal formulations for once daily application of etamsylate. Moreover, prediction of the *in-vivo* plasma profile was conducted using a simple convolution method. The prediction of *in-vivo* pharmacokinetic of etamsylate was very useful to understand the applicability of the designed matrices in humans however, further *in-vivo* study should be performed in the future on selected matrices to compare the predicted plasma concentrations with the actual ones.

Declaration of Competing Interest

The authors declare that they have no known competing financial interests or personal relationships that could have appeared to influence the work reported in this paper.

Acknowledgements

The authors want to thank Dr Saeed Qureshi for his valuable help.

References

- Aigner, Z., Heinrich, R., Sipos, E., Farkas, G., Ciurba, A., Berkesi, O., Szabó-Révész, P., 2011. Compatibility studies of aceclofenac with retard tablet excipients by means of thermal and FT-IR spectroscopic methods. *J. Therm. Anal. Calorim.* 104, 265–271.
- Alderman, D.A., 1984. A review of cellulose ethers in hydrophilic matrices for oral controlled-release dosage forms. *Int. J. Pharm. Tech. Prod. Mfr.* 5, 1–9.
- Bendas, E.R., 2009. Two different approaches for the prediction of in vivo plasma concentration–time profile from in vitro release data of once daily formulations of diltiazem hydrochloride. *Arch. Pharm. Res.* 32 (9), 1317–1329.
- Bettini, R., Catellani, P.L., Santi, P., Massimo, G., Peppas, N.A., Colombo, P., 2001. Translocation of drug particles in HPMC matrix gel layer: effect of drug solubility and influence on release rate. *J. Control. Rel.* 70 (3), 383–391.
- Bhat, V., Shivakumar, H.R., Sheshappa, R.K., Sanjeev, G., 2014. Preparation and study on miscibility, thermal behavior of biocompatible polymer blends of xanthan Gum-polyacrylamide. *Int. J. Plast. Technol.* 18, 183–191.
- British Pharmacopoeia (BP), 2000. 636–637.
- British Pharmacopoeia (BP), 2004. Vol. 2, London: The Stationary office.
- Carr, R.L., 1965. Classifying flow properties of solids. *Chem. Eng.* 72, 69–72.
- Center for Drug Evaluation and Research (CDER), 1997. Guidance for Industrial Extended Release Oral Dosage Forms: Development, Evaluation and Application of In Vitro/In Vivo Correlations. Food and Drug Administration, Rockville, MD.
- Chaibva, F.A., Khamanga, S.M., Walker, R.B., 2010. Swelling, erosion and drug release characteristics of salbutamol sulfate from hydroxypropyl methylcellulose-based matrix tablets. *Drug Dev. Ind. Pharm.* 36 (12), 1497–1510.
- Chateau, M.E., Galet, L., Soudais, Y., Fages, J., 2005. Processing a detergent powder formulation: Direct compression, and high shear wet granulation followed by compression. *Powder Tech.* 157, 191–198.
- Costa, P., Lobo, J., 2001. Modeling and comparison of dissolution profiles. *Eur. J. Pharm. Sci.* 13, 123–133.
- Costa, P., 2001. An alternative method to the evaluation of similarity factor in dissolution testing. *Int. J. Pharm.* 220, 77–83.
- Desai, S.R., Shaikh, M.M., Dharwadkar, S.R., 2003. Preformulation compatibility studies of etamsylate and fluconazole with lactose by DSC. *J. Therm. Anal. Cal.* 71, 651–658.
- DiColo, G., Baggiani, A., Zambito, Y., Mollica, G., Geppi, M., Serafini, M.F., 2006. A new hydrogel for the extended and complete prednisolone release in the GI tract. *Int. J. Pharm.* 310, 154e161.
- Dorozynski, P., Jachowicz, R., Kulinowski, P., Kwiecinski, S., Szybinski, K., Skorka, T., Jasinski, A., 2004. The polymers for the preparation of hydrodynamically balanced systems – methods of evaluation. *Drug Dev. Ind. Pharm.* 30 (9), 947–957.
- Dunne, A., O'Hara, T., Devane, J., 1997. Level A in vivo-in vitro correlation: Nonlinear models and statistical methodology. *J. Pharm. Sci.* 86, 1245–1249.
- European agency for the evaluation of medicinal products (EMA), 1998. Committee for veterinary pharmaceutical products. Etamsylate. Summary report. <https://www.ema.europa.eu/en/documents/mrl-report/etamsylate-summary-report-committee-veterinary-medicinal-products.en.pdf> [last accessed 18th August 2020].
- European Pharmacopoeia (EP), 2008. 6.0 6th Edition. Etamsylate. <http://www.uspbep.com/ep60/etamsylate%201204e.pdf> [accessed 20 August 2020].
- Ford, J.L., 1999. Thermal analysis of hydroxypropylmethylcellulose and methylcellulose: powders, gels and matrix tablets. *Int. J. Pharm.* 179 (2), 209–228.
- Ford, J.L., Rubenstein, M.H., Hogan, J.E., 1985. Propranolol hydrochloride and aminophylline release from matrix tablets containing hydroxypropyl methylcellulose. *Int. J. Pharm.* 24, 339–350.
- Garay, R.P., Chiavaroli, C., Hannaert, P., 2006. Therapeutic efficacy and mechanism of action of etamsylate, a long-standing hemostatic agent. *Am. J. Ther.* 13 (3), 236–247.
- Garg, R., Gupta, G.D., 2009. Preparation and evaluation of gastroretentive floating tablets of Silymarin. *Chem. Pharm. Bull.* 57 (6), 545–549.
- Ghori, M.U., Ginting, G., Smith, A.M., Conway, B.R., 2014. Simultaneous quantification of drug release and erosion from hypromellose hydrophilic matrices. *Int. J. Pharm.* 465, 405–412.
- Ginski, M.J., Polli, J.E., 1999. Prediction of dissolution absorption relationships from a dissolution/Caco-2 system. *Int. J. Pharm.* 177, 117–125.
- Gohel, M.C., Parikh, R.K., Brahmabhatt, B.K., Shah, A.R., 2007. Improving the tablet characteristics and dissolution profile of ibuprofen by using a novel coprocessed superdisintegrant: a technical note. *AAPS PharmSciTech.* 8 (1), Article 13.
- Hedaya, M.A., 2012. Basic pharmacokinetics. In: Taylor and Francis, editor. Taylor and Francis group; 6000 Broken Sound Parkway NW, Suit 300, Boca Raton, FL 33487-2742, England.
- Helmy, S.A., El Bedaiwy, H.M., 2013. A new and simple HPLC method for determination of etamsylate in human plasma and its application to pharmacokinetic study in healthy adult male volunteers. *Saudi Pharm. J.* 21 (4), 405–410.
- Helmy, S.A., ElBedaiwy, H.M., 2016. In Vitro dissolution similarity as a surrogate for in vivo bioavailability and therapeutic equivalence. *Dissolut. Technol.* 23 (3), 32–39.
- Hidekatsu, N., Chiaki, H., Tetsuya, A., Ichiro, O., Yuji, M., Susumu, N., Kazuhisa, T., Yuji, K., 2007. Application of the correlation of in vitro dissolution behavior and in vivo plasma concentration profile (IVIVC) for soft-gel capsules—a pointless pursuit?. *Biol. Pharm. Bull.* 30 (11), 2221–2225.
- Higuchi, T., 1963. Mechanism of sustained-action medication. Theoretical analysis of rate of release of solid drugs dispersed in solid matrices. *J. Pharm. Sci.* 52, 1145–1149.
- Hussein, Z., Friedman, M., 1990. Release and absorption characteristics of novel theophylline sustained-release formulations. In vitro-in vivo correlation. *Pharm. Res.* 7, 1167–1171.
- Hwang, S.S., Gorsline, J., Louie, J., Dye, D., Guinta, D., Hamel, L., 1995. In vitro and in vivo evaluation of a once-daily controlled-release pseudoephedrine product. *J. Clin. Pharmacol.* 35, 259–267.
- International Conference on Harmonisation of Technical Requirements for Registration of Pharmaceuticals for Human Use. ICH Harmonised Tripartite Guideline: Stability testing: photostability testing of new drug substances and products Q1B, 1996. Available from: https://database.ich.org/sites/default/files/Q1B_Guideline.pdf [accessed 20 August 2020].
- Juarez, H., Rico, G., Villafuerte, L., 2001. Influence of admixed carboxymethylcellulose on release of 4-aminopyridine from hydroxypropyl methylcellulose matrix tablets. *Int. J. Pharm.* 216, 115–125.
- Khan, G.M., Jiabi, Z., 1998. Formulation and in vitro evaluation of ibuprofen-Carbopol 974P-NF controlled release matrix tablets. II: Influence of co-excipients on release rate of the drug. *J. Control. Rel.* 54, 185–190.
- Khan, K.A., 1975. The concept of dissolution efficiency. *J. Pharm. Pharmacol.* 27, 48–49.
- Khanum, H., Ullah, K., Murtazab, G., AliKhana, S., 2018. Fabrication and in vitro characterization of HPMC-g-poly(AMPS) hydrogels loaded with loxoprofen sodium. *Int. J. Bio. Macromolecules* 120 B, 1624–1631.
- Korsmeyer, R.W., Gurny, R., Doelker, E., Buri, P., Peppas, N.A., 1983. Mechanisms of solute release from porous hydrophilic polymers. *Int. J. Pharm.* 15, 25e35.
- Kumar, V., Kothari, S.H., Banker, G.S., 2001. Compression, compaction, and disintegration properties of low crystallinity celluloses produced using different agitation rates during their regeneration from phosphoric acid solutions. *AAPS PharmSciTech.* 2 (2), Article 7.
- Li, C.L., Martini, L.G., Ford, J.L., Roberts, M., 2005. The use of hypromellose in oral drug delivery. *J. Pharm. Pharmacol.* 57 (5), 533–546.
- Maderuelo, C., Zarzuelo, A., Lanao, J.M., 2011. Critical factors in the release of drugs from sustained release hydrophilic matrices. *J. Control. Release.* 154 (1), 2–19.
- Mathews, B.R., 1999. Regulatory aspects of stability testing in Europe. *Drug Dev. Ind. Pharm.* 25, 831–856.
- Mitchell, K., Ford, J.L., Armstrong, D.J., Elliott, P.N.C., Rostron, C., Hogan, J.E., 1993. The influence of concentration on the release of drugs from gels and matrices containing Methocel®. *Int. J. Pharm.* 100 (1–3), 155–163.
- Mojaverian, P., Radwanski, E., Lin, C.C., Cho, P., Vadino, W.A., Rosen, J.M., 1992. Correlation of in vitro release rate and in vivo absorption characteristics of four chlorpheniramine maleate extended-release formulations. *Pharm. Res.* 9, 450–456.
- Moore, J.W., Flanner, H.H., 1996. Mathematical comparison of dissolution profiles. *Pharm. Tech.* 20, 64–74.
- Nep, E.L., Conway, B.R., 2012. Preformulation studies on grevia gum as a formulation excipient. *J. Therm. Anal. Calorim.* 108, 197–205.
- Paroiea, J., Ibrăe, S., Djurică, Z., Jovanović, M., Corrigan, O.I., 2007. An investigation into the usefulness of generalized regression neural network analysis in the development of level A in vitro-in vivo correlation. *Eur. J. Pharm. Sci.* 30, 264–272.
- Patel, A., Modasiya, M., Shah, D., Patel, V., 2009. Development and in vivo floating behavior of verapamil HCl intragastric floating tablets. *AAPS PharmSciTech.* 10 (1), 310–315.
- Peppas, N.A., 1985. Analysis of Fickian and non-Fickian drug release from polymers. *Pharm. Acta. Helv.* 60, 110–111.
- Podczec, F., 1993. Comparison of in vitro dissolution profiles by calculating mean dissolution time (MDT) or mean residence time (MRT). *Int. J. Pharm.* 97 (1–3), 93–100.
- Polli, J.E., Crison, J.R., Amidon, G.L., 1996. Novel approach to the analysis of In vitro relationships. *J. Pharm. Sci.* 85, 753–759.
- Prajapati, S., Patel, L., Patel, C., 2011. Floating matrix tablets of domperidone formulation and optimization using simple lattice design. *Iran. J. Pharm. Res.* 10 (3), 447–455.
- Qureshi, S.A., 2010. In vitro-in vivo correlation (IVIVC) and determining drug concentrations in blood from dissolution testing – a simple and practical approach. *Open Drug Deliv. J.* 4, 38–47.
- Ramasamy, T., Kandhasami, U.D.S., Ruttala, H., Shanmugam, S., 2011. Formulation and evaluation of xanthan gum based aceclofenac tablets for colon targeted drug delivery. *Braz. J. Pharm. Sci.* 47 (2), 299–311.
- Rao, P.R., Kotreka, U.K., Saha, R.N., 2008. Controlled release matrix tablets of zidovudine: effect of formulation variables on the in vitro drug release kinetics. *AAPS PharmSciTech.* 9, 302–312.
- Reza, M.S., Abdul Quadir, M., Haider, S.S., 2003. Comparative evaluation of plastic, hydrophobic and hydrophilic polymers as matrices for controlled-release drug delivery. *J. Pharm. Pharm. Sci.* 6 (2), 282–291.
- Ritger, R.L., Peppas, N.A., 1987. A simple equation for the description of solute release. II. Fickian and anomalous release from swellable devices. *J. Control. Rel.* 5, 37–42.
- Salsa, T., Veiga, F., Pina, M.E., 1997. Oral controlled-release dosage forms. I. Cellulose ether polymers in hydrophilic matrices. *Drug Dev. Ind. Pharm.* 23, 929–938.
- Samani, S.M., Montaseri, H., Kazemi, A., 2003. The effect of polymer blends on release profiles of diclofenac sodium from matrices. *Eur. J. Pharm. Biopharm.* 55, 351–355.

- Sankalia, J.M., Sankalia, M.G., Mashru, R.C., 2008. Drug release and swelling kinetics of directly compressed glipizide sustained-release matrices: Establishment of level A IVIVC. *J. Control. Rel.* 129, 49–58.
- Schulte, J., Osborne, J., Benson, J., Cooke, J.W., Drayton, R., Murphy, M., Rennie, J., Speidel, J., 2005. Developmental outcome of the use of etamsylate for prevention of periventricular haemorrhage in a randomized controlled trial. *Arch. Dis. Child. Fetal Neonatal Ed.* 90 (1), F31–F35.
- Seng, C.H., Hasaesum, P., Peggy, K., Robinson, J.R., 1985. Bioadhesive polymers as platforms for oral controlled release drug delivery II: Synthesis and evaluation of some swelling, water-insoluble bioadhesive polymers. *J. Pharm. Sci.* 74, 399–405.
- Shah, N., Zhang, G., Apelian, V., Zeng, F., Infeld, M.H., Malick, A.W., 1993. Prediction of drug release from hydroxypropyl methylcellulose (HPMC) matrices: effect of polymer concentration. *Pharm. Res.* 10, 1693–1695.
- Shah, R.B., Tawakkul, M.A., Khan, M.A., 2008. Comparative evaluation of flow for pharmaceutical powders and granules. *AAPS PharmSciTech.* 9 (1), 250–258.
- Siepmann, J., Peppas, N.A., 2001. Modeling of drug release from delivery systems based on hydroxypropyl methylcellulose (HPMC). *Adv. Drug Deliv. Rev.* 48, 139–157.
- Siepmann, J., Siepmann, F., 2013. Mathematical modeling of drug dissolution. *Int. J. Pharm.* 453 (1), 12–24.
- Singhvi, G., Shah, A., Yadav, N., Saha, R.N., 2014. Study the effect of formulation variables on drug release from hydrophilic matrix tablets of milnacipran and prediction of in-vivo plasma profile. *Pharm. Dev. Technol.* 19 (6), 708–716.
- Sinha Roy, D., Rohera, B., 2002. Comparative evaluation of rate of hydration and matrix erosion of HEC and HPC and study of drug release from their matrices. *Eur. J. Pharm. Sci* 16 (3), 193–199.
- Spoljaric, S., Genovese, A., Shanks, R.A., 2009. Polypropylene microcrystalline cellulose composites with enhanced compatibility and properties. *Compos. Part A* 40, 791–799.
- Staniforth, J.N., 2002. Powder flow. In: Aulton, M.E. (Ed.), *Pharmaceutics. The Science of Dosage Form Design*. Churchill Livingstone, pp. 197–210.
- Tadros, M.I., 2010. Controlled-release effervescent floating matrix tablets of ciprofloxacin hydrochloride: Development, optimization and in vitro-in vivo evaluation in healthy human volunteers. *Eur. J. Pharm. Biopharm.* 74 (2), 332–339.
- Talukdar, M.M., Kinge, R., 1995. Swelling and drug release behavior of xanthan gum matrix tablets. *Int. J. Pharm.* 120 (1), 63–72.
- Thoorens, G., Krier, F., Leclercq, B., Carlin, B., Evrard, B., 2014. Microcrystalline cellulose, a direct compression binder in a quality by design environment – a review. *Int. J. Pharm.* 473 (1), 64–72.
- United States Pharmacopeia National Formulary 38 (USP-NF 38), 2014. United States Pharmacopial Convention, Rockville, MD.
- Velasco, M.V., Ford, J.L., Rowe, P., Rajabi-Siahboomi, A.R., 1999. Influence of drug: hydroxypropyl methylcellulose ratio, drug and polymer particle size and compression force on the release of diclofenac sodium from HPMC matrices. *J. Control. Rel.* 57, 75–85.
- Venugopalarao, G., Sreenivas Gowtham, M., Sarada, N.C., 2013. Formulation evaluation and stability studies of hydrogel tablets containing Cefditoren Pivoxil. *J. Pharm. Res.* 7 (3), 230–234.
- Wan, L.S.C., Heng, P.W.S., Wongh, L.F., 1991. The effect of hydroxypropyl methylcellulose on water penetration into a matrix system. *Int. J. Pharm.* 73, 111–116.
- Yang, L., Fassihi, R., 1997. Examination of drug solubility, polymer types, hydrodynamics and loading dose on drug release behavior from a triple-layer asymmetric configuration delivery system. *Int. J. Pharm.* 155 (2), 219–229.
- Zhang, Y., Huo, M., Zhou, J., Zou, A., Li, W., Yao, C., Xie, S., 2010. DDSolver: an add-in program for modeling and comparison of drug dissolution profiles. *AAPS J.* 12 (3), 263–271.